Synthesis, Spectral Characterisation and Biological Evaluation of a New Azo-Ligand Derived from Aminoacetophenone with its Metal Complexes

Mohammed Qays Mezher and Enaam Ismail Yousif
Department of Chemistry, College of Education for Pure Science, University of Baghdad, 10071 Baghdad, Iraq
anaam.i.y@ihcoedu.uobaghdad.edu.iq,mohammed.qais2205@ihcoedu.uobaghdad.edu.iq

Keywords: (E)-3-((4-Acetylphenyl)Diazenyl)-2-Hydroxy-1-Naphthaldehyde, Metal Complexes, Azo Ligand, Proteus Mirabilis, 4-Aminoacetophenone.

Abstract: Synthesis and characterisation of a new azo ligand based on a 4-aminoacetophenone moiety, along with its metal complexes. The synthesis of the ligand, ((E)-3-((4-acetylphenyl)diazenyl)-2-hydroxy-1-naphthaldehyde) (HL), was obtained from the interaction of 4-aminoacetophenone with 2-hydroxynaphthalene-1-carbaldehyde in a one-to-one molar ratio. Subsequently, the interaction of HL with various metal ions (Cr(III), Mn(II), Co(II), Ni(II) and Cu(II) in the ratio of one ligand to one metal, produced monomeric coordination connections. These compounds have been fully characterised using analytical methods and spectroscopic techniques, involve elemental microanalysis,^{1}H and ^{13}C-nuclear magnetic resonance, Fourier transform infrared spectroscopy, electronic and mass spectroscopy, as well as magnetic susceptibility and Conductivity measurements. The analytical data verified the formation of coordination compounds exhibiting six-coordinate geometries. The antibacterial evaluation of the ligand and its coordination complexes against bacterial strains and fungus species showed a significant enhancement in the effectiveness of the antimicrobial ligand when forming complexes with metal ions. In addition, the study evaluated the antibacterial activity of synthesised compounds with a number of bacteria and fungi. The complex formation significantly enhanced the antibacterial efficacy of the ligand.

1 INTRODUCTION

The chemical compounds characterised by the functional group RN=NR called Azo dyes′, where R and R′ are typically aryl groups [1]. It is frequently used to create mono-azo dyes, which are marketed as coloring agents [2]-[6]. They could include [1]-[3] azo linkages connecting phenol group and naphthalene. Strong colours distinguish azo dyes, they are thought to constitute the majority of the synthetic dyes generated today. This class of commercially available organic dyes has the highest structural variety and a wide range of uses [7], [8]. Azo dyes are primarily synthesised through the diazotisation of a primary amine, followed by conjugation with one or more electron-rich nucleophiles, including amines or hydroxyl groups [9]. Azo dyes have special characteristics, including molecular aggregation and optical data storage capacity. In addition, they have been used in various fields of activity, such as textile fibre colouring, plastic, leather, metal chips, food products, cosmetics, toys, plastics, biological and clinical research, and even organic composition [10], [11]. Azo-dyes exhibit biological activity, including antibacterial, antifungal, anti-HIV, and anticancer properties. Therefore, they are of enormous importance in medical chemistry [12], [13]. A considerable amount of work was devoted to the advancement and characterisation of excellent azohydroxyl ligands, which possess the capability to chelate metal ions and create complexes with different configurations of structures [14]. In recent years, we have documented the production of azo chemicals and the complexes they create [15]-[17]. This chemical interaction of 2-hydroxynaphthalene-1-carbaldehyde with 4-aminoacetophenone generated the ligand. The produced compounds' antimicrobial and antifungal properties were also examined.

2 MATERIALS AND EXPERIMENTAL PROCEDURES

The ligand's nuclear magnetic resonance spectra, which include (^{1}H and ^{13}C) spectrum, Utilising dimethyl sulfoxide-d6 as the solvent, the results have been obtained with a Bruker 400 MHz spectrometer. The measurement frequencies had been 400 MHz for ^{1}H and 100 MHz to obtain ^{13}C, using tetramethylsilane as the internal standard. Fourier transform infrared spectroscopy The spectrum has been obtained utilising KBr granules and collected by using the FTIR-600 infrared Fourier spectrometer throughout a spectrum range of 4000 to 200 cm^{-1}. Analyses utilising positive ion electrospray mass spectrometry were performed with a Sciex ESImass spectrometer. We used a Stuart SMP4 electrothermal device to determine the melting points of compounds. The spectrum of UV-visible has been obtained within the wavelength range of 1000 to 200 nm utilising a Shimadzu UV-160A spectrophotometer. At room temperature, using dimethyl sulfoxide, the solutions were prepared at a concentration of 10^{-3} mol L^{-1} and analysed in a one-centimetre quartz cuvette. The Eutech Instruments Cyber Can CON 510 digital conductivity meter was employed to determine the conductivity of the solution in DMSO with concentrations between 10^{-1} and 10^{-5}. At the Heraeus Vario EL and Shimadzu AA-7000 atomic absorption, elemental (C, H, N) and metal content were utilised for the analysis. Utilising a Metrohm 686 Titro processor and a 665 Dosim unit, the quantification for chloride ions in compounds was conducted by potentiometric titration. Finally, using a magnetic balance from Johnson Matthey, the magnetic characteristics have been assessed at 30°C.

3 SYNTHESIS

3.1 Synthesis of ((E)-3-((4-Acetylphenyl) Diazenyl)-2-Hydroxy-1-Naphthaldehyde) (HL)

Preparation of HL was based on the described method [18]-[20] as follows; In a 250 ml round flask containing 1.35g (10 mmol) of 4-aminoacetophenone and 0.69g (10 mmol) of sodium nitrite, 20 ml of one-to-one (EtOH:H_2O) mixture was added. The mixture was cooled to a temperature range of 0 to 5°C in an ice bath. Subsequently, 3 ml of hydrochloric acid (36%) was placed in a beaker with 10 ml of cold distilled water, then added dropwise with stirring over one hour. Diazonium salt solution is the product of this process, then reacts with a coolant mix that has 0.8g (20mmol) of sodium hydroxide and 1.72g (10 mmol) of 2-hydroxynaphthalene-1-carbaldehyde in 20ml of ethanol. The mixture of reaction was allowed to stir for two hours. Following to the reaction, the precipitate had been filtrated at pH 4, washed with cold water until its pH became 6-7, and then allowed to dry. The precipitate was filtered and was orange-red in colour. The precipitate was washed with 5 ml of cold ethanol and then allowed to dry. The yield: 2.293g (72.10%), having a melting point among 136-138°C (Fig. 1). ^{1}H nuclear magnetic resonance (400 MHz,DMSO-$_6$,ppm). $H_{(a)}$ at δ 9.67 ppm. 8.54; 8.45 ppm (s, 1H), which equivalent to $H_{(b)}$ and $H_{(c)}$ protons, respectively. $H_{(g.g-)}$ at 8.33 (d, J = 9.1 Hz, 2H). $H_{(h,h-)}$ displays at 7.79 (d, J = 7.9 Hz, 2H). $H_{(d,f)}$ at 7.48, 7.39 (t, J = 7.5 Hz, 2H). at 7.01 (d, J = 9.2 Hz, 2H); 6.76 (d, J = 9.6 Hz, 1H) belongs to $H_{(j,k)}$. $H_{(i)}$ at 2.60 ppm. Finally, at 15.27 ppm belongs to the impact of tautomerism. The ^{13}C-nuclear magnetic resonance (100 MHz, DMSO-d_6, ppm). Resonances at δ_c = 197.11 and 193.27 ppm were assigned to carbonyl carbon: (ketonic C_a); (aldehydic C_b), respectively. The Signal of phenolic carbon (C_c) was detected at 177.23 ppm. Resonances assigned for N- (C_n), was observed at 164.44 ppm, when the other N- (C_q) chemical shifts appeared at 147.06 ppm. The two signals displayed at 143.02; 138.89 were related to (C_w), (C_t), respectively. The peaks which related to (C_e), (C_x) and (C_k) showed with 134,54; 132.14; 130.62 ppm frequency respectively. The two groups of Carbon nucleuses of ($C_{g,g-}$); ($C_{h,h-}$), assigned at 129.75 and 124.71 ppm. Resonance of (C_u); (C_d) signals appears at 128.61; 122.71 ppm, respectively. The assignments of (C_f) and (C_j) resonance appeared at 117.70 and 119.20 ppm, respectively. The methyl group (C_m), appeared as a one peak at 27.15 ppm.

3.2 Synthesis of Complexes

The synthesised complexes process was a similar process used to synthesise the chromium(III) complex. The process will be as follows: It has been placed 0.3g (0.94 mmol) of HL has been dissolved in 10 ml in a mixed solution (5:5) (ethanol-benzene), and then 10ml of ethanol solution KOH 0.05g (0.94 mmol) was added in a 100 ml round-bottomed flask.

We stirred the mix. Subsequently, the slow addition of a solution of Chromium(III) chloride hexahydrate 0.25g (0.94 mmol) in 5 ml of EtOH was performed. The reaction mixture had been subjected to reflux heating for two hours. Following the heat process, the substance underwent filtration, washed to remove any remaining unreacted material used a cold ethanol and allowed to air dry. 0.262g (60.83%) was the yield of the Cr(III) complex, with a melting point above 300°C. The synthesis process has been described in Figure 2. See Table 1 for further information on yields, colors, the amounts of metal salts utilised, and m.p. of the resulting complexes.

4 MICROBIOLOGICAL EVALUATION

The susceptibility of bacteria and fungi to the generated chemicals has been assessed utilising the Kirby-Bauer disk diffusion method. Organism colonies were suspended in an 85% sodium chloride solution to achieve a turbidity comparable to 0.5 McFarland standard. over the surface of Mueller Hinton agar in a Petri dish, this suspension was evenly spread. Wells on the agar were created with uniform spacing and concentration. In each well, 100 ml of the test sample diluted to 1 mg/ml DMSO was added. After incubating, zones of inhibition were evaluated for 24 hours at 37°C and compared to reference values [21]. Control experiments using DMSO solutions confirmed the absence of intrinsic anti-microbial activity. Any of the tested bacteria or fungus.

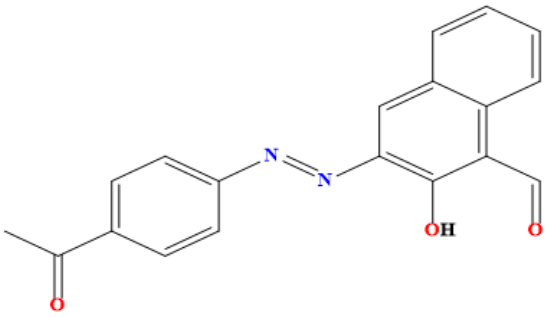

Figure 1: Chemical structure of azo ligand.

Table 1: Yield, colors, metal salts quantites and m.p. of ligand complexes.

Complexes	Quantity of metal salts (g)	Quantity of complex(g)	Colors	m.pºC	Yield (%)
$[Cr(L)Cl_2H_2O]$	0.25	0.43	Yellowish-green	>300*	60.83
$[Mn(L)Cl(H_2O)_2]$	0.19	0.42	Dark orange	>300*	70.00
$[Co(L)Cl(H_2O)_2]$	0.22	0.42	Dark brown	>300*	75.82
$[Ni(L)Cl(H2O)_2]$	0.22	0.42	Dark green	>300*	79.14
$[Cu(L)Cl(H_2O)_2]$ *=Decomposed	0.23	0.43	Reddish-brown	>300*	66.38

Table 2: Microanalysis and physical characteristics of complexes.

Complexe	Molecular formula	M.Wt	Microanalysis found, (calculated) %				
			C	H	N	M	Cl
$[Cr(L)Cl_2H_2O]$	$C_{19}H_{15}Cl_2CrN_2O_4$	458.27	(49.80) 49.51	(3.30) 3.13	(6.11) 6.00	(11.35) 11.11	(15.47) 15. 05
$[Mn(L)Cl(H_2O)_2]$	$C_{19}H_{17}ClMnN_2O_5$	443.74	(51.43) 51.24	(3.86) 3.40	(6.31) 6.01	(12.38) 12.05	(7.99) 7.61
$[Co(L)Cl(H_2O)_2]$	$C_{19}H_{17}ClCoN_2O_5$	447.74	(50.97) 50.67	(3.83) 3.53	(6.26) 6.12	(13.16) 13.01	(7.92) 7.70
$[Ni(L)Cl(H_2O)_2]$	$C_{19}H_{17}ClNi\ N_2O_5$	447.50	(51.00) 50.87	(3.83) 3.62	(6.26) 6.15	(13.12) 13.00	(7.92) 7.41
$[Cu(L)Cl(H_2O)_2]$	$C_{19}H_{17}ClCuN_2O_5$	452.35	(50.45) 50.23	(3.79) 3.56	(6.19) 6.01	(14.05) 13.88	(7.84) 7.67

5 RESULTS AND DISCUSSION

The azo ligand ((E)-3-((4-acetylphenyl)diazenyl)-2-hydroxy-1-naphthaldehyde) (HL). In this approach, $NaNO_2$, HCl and EtOH were used as a catalyst and reaction medium, respectively.4-aminoacetophenone and 2-hydroxynaphthalene-1-carbaldehyde reacting in EtOH at a one-to-one ratio. The ligand functions as a tridentate species, supplying the azo's nitrogen atom, hydroxyl, and carbonyl oxygen as donor atoms. The interaction of the ligand with the chlorides of metal of Cr(III), Mn(II), Co(II), Ni(II), and Cu(II) occurs in a mole ratio of one to one (Ligand to Metal) yielded the segregation of six-coordinate monomeric compound of the universal formula $[M(L)Cl_2H_2O]$ with Cr(Ш), $[M(L)Cl(H_2O)_2]$ with Mn(II) and Cu(II), Co(II) and Ni(II) ions (Figure 2). The isolated compounds exhibit stability in the air, exist as solids, and are soluble in DMSO and DMF. However, it is not soluble in other common organic solvents. Based on their physico-chemical data, complexes' coordination geometries and complexation behavior were assumed. Results shown in Table 2 are well suited to the proposed formula. Conductance measurements of the compounds in dimethylsulfoxide solutions showed that the complexes are non-electrolytic. The entity of Azo was confirmed by C, H, N, M (Table 2), Fourier transform infrared spectroscopy (Table 3), and Electron spectroscopy (Table 4).

5.1 FT-IR and NMR Data

In Table 3, the main IR absorption bands of the complexes are listed with their duties. The peak is observable in the ligand spectrum at 3194 cm^{-1} due to ν(OH) stretching vibration of the phenol hydroxyl group [22]. at 1621 and 1492 cm^{-1}. The noted bands correspond to the stretching of the carbonyl group ν(C=O) and the stretching of the azo group ν(N=N), respectively [23]. The complex spectrum had a noticeable extent between 1617 and 1612 cm^{-1}.which is related to the ν (C=O) stretching vibration. The ligand's spectra appeared the band at 1621 cm^{-1}. Interaction involving the metal ion and the carbonyl oxygen atom is explained by the bands that form upon complexation [22]. Band observed at 1492 cm^{-1} in HL, which belongs to the azo group ν(N=N) [20], [22]. It was displaced and appeared at 1463, 1466, 1489, 1465, and 1465 cm^{-1} in the five complexes in order. The occurrence might have been associated with the involvement of the nitrogen atom in complexation. In addition, the metal complex spectra revealed new bands around (646-629), (464-419), and (289-223) cm^{-1} that were not visible in the ligand spectrum associated to ν(M-O), ν(M-N), and ν(M-Cl), respectively [22], [23]. Finally, the complexes of Cr(Ш), Mn(II), Co(II), Ni(II), and Cu(II) showed peaks at (3439), (3432), (3337), (3450), and (3547) cm^{-1}, respectively. were bound to aqua molecules. At 742, 749, 756, 740, and 742 cm^{-1}, complex bands 1, 2, 3, 4, and 5 can be found. These are linked to water-coordinated ν(M-O) for 1,2,3,4 and 5 [20], [25]. The identification of peaks in the nuclear magnetic resonance spectra corresponds to the numbering scheme shown in Figure 1. The spectra ^1H nuclear magnetic resonance of ligand with dimethyl sulfoxide (d_6) as a solvent, is shown in Figure 3. The chemical shift at δ 9.67 ppm (s, 1H), that equivalent to one proton attributed to phenolic proton $H_{(a)}$. The chemical shift that appeared as a singlet signal at 8.54; 8.45 ppm (s, 1H), which equivalent to $H_{(b)}$ and $H_{(c)}$ protons, respectively. The spectrum shows doublet signal refers to $H_{(g.g-)}$ at 8.33 (d, J = 9.1 Hz, 2H). The doublet signal of attributed to $H_{(h,h-)}$ displays at 7.79 (d, J = 7.9 Hz, 2H). The value of $H_{(d,f)}$ appear as a triplet signal at 7.48, 7.39 (t, J = 7.5 Hz, 2H). when another doublets signals displayed at 7.01 (d, J = 9.2 Hz, 2H); 6.76 (d, J = 9.6 Hz, 1H) belongs to $H_{(j,k)}$ protons. The aliphatic region revealed a singlet peak belongs to $H_{(i)}$ protons appeared at 2.60 ppm. At 2.51 and 3.37 ppm, peaks were seen corresponding to the dimethyl sulfoxide-d_6 solvent and trace water molecules present in the solvent, respectively. Finally, the proton signal which appeared at a very low chemical shifting area, near 15.27 ppm belongs to the impact of tautomersim which phenols suffer from [26]-[29]. Obesely the spectrum don't displays a signals between 4-5 ppm which proven the transformation of amine group to diazo moiety. Figure 4 shows the ^{13}C nuclear magnetic resonance spectrum in DMSO-d_6, which shows the correct number of carbon atoms in a molecule. Resonances at δ_c = 197.11 and 193.27 ppm were assigned to carbonyl carbon: (ketonic C_a); (aldehydic C_b), respectively. The Signal of phenolic carbon (C_c) was detected at 177.23 ppm. Resonances assigned for N- (C_n), was observed at 164.44 ppm, when the other N- (C_q) chemical shifts appeared at 147.06 ppm. The two signals displayed at 143.02; 138.89 were related to (C_w), (C_t), respectively. The peaks which related to (C_e), (C_x) and (C_k) showed with 134,54; 132.14; 130.62 ppm frequency respectively. The two groups of Carbon nucleuses of ($C_{g,g-}$); ($C_{h,h-}$), assigned at 129.75 and 124.71 ppm. Resonance of (C_u); (C_d) signals appears at 128.61;

122.71 ppm, respectively. The assignments of (C_f) and (C_j) resonance appeared at 117.70 and 119.20 ppm, respectively. The methyl group (C_m), appeared as a one peak at 27.15 ppm, when the solvent signals of the DMSO-d_6 resonances appeared at 40.50-39.33.

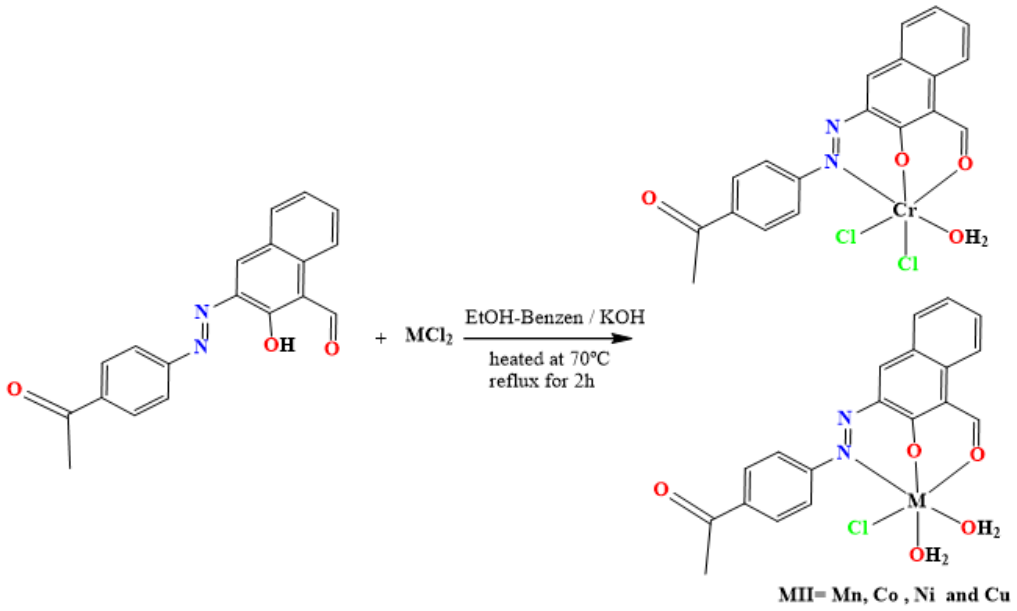

Figure 2: General route for the synthesis of HL complexes.

Table 3: FT-IR data of the most prominent peaks of complexes (cm^{-1}).

Compounds	ν(C=O) ke ν(C=O)al	ν (C=C)	ν N=N	ν C-O ν C-N	ν(H_2O) ν(M-OH_2)	ν (M-O) phenol ν (M-O) aldeh.	ν M-N	ν M-Cl
$C_{19}H_{15}Cl_2CrN_2O_4$	1674 1612	1593 1544 1500	1463	1357 1265	3439 742	646 590	464	279 260
$C_{19}H_{17}ClMnN_2O_5$	1671 1617	1597 1581 1538	1466	1357 1261	3432 749	629 536	449	281
$C_{19}H_{17}ClCoN_2O_5$	1674 1615	1598 1577 1558 1551	1489	1334 1262	3337 756	629 558	419	262
$C_{19}H_{17}ClNiN_2O_5$	1674 1614	1593 1543 1500	1465	1355 1267	3450 740	623 572	451	289
$C_{19}H_{17}ClCuN_2O_5$	1678 1614	1593 1544 1502	1465	1357 1265	3547 742	646 569	420	223

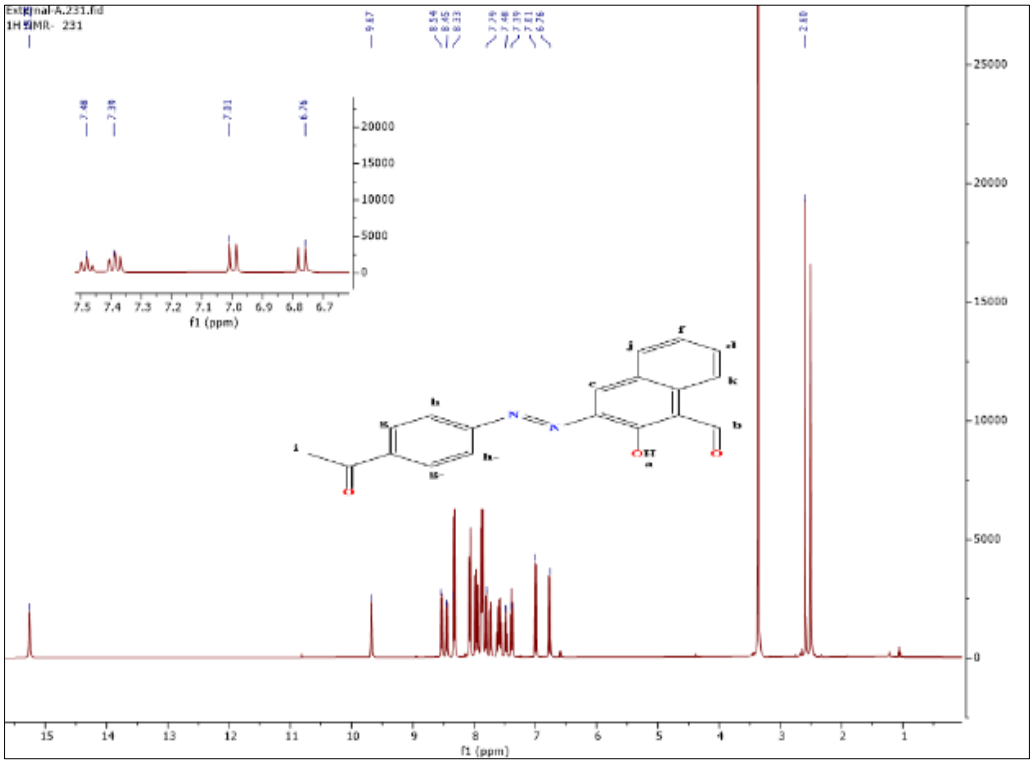

Figure 3: ^{1}H-NMR spectrum in DMSO-d_6 solutions of azo ligand.

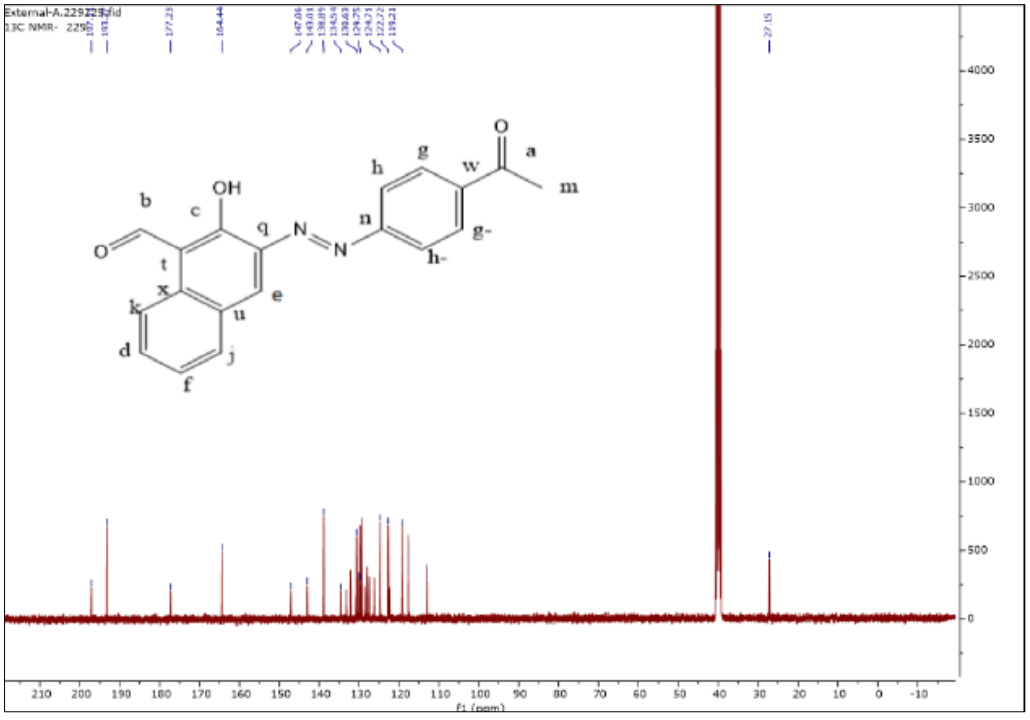

Figure 4: ^{13}C-NMR spectrum in DMSO-d_6 solutions of azo ligand.

Table 4: Uv-vis data for complexes in DMSO solutions.

Complex	ʎnm	Molar extinction coefficient εmax (dm^3 mol^{-1} cm^{-1})	Assignment	Suggested geometry
$C_{19}H_{15}Cl_2CrN_2O_4$	301 436 512	1760 597 22	Intra-ligand π → π*, n→π* C.T $^4A_2g \rightarrow {}^4T_1g^{(p)}$	Distorted octahedral
$C_{19}H_{17}ClMnN_2O_5$	287 316 374 401 488	1090 771 559 459 85	Intra-ligand π → π*, n→π* C.T C.T C.T $^6A_1g \rightarrow {}^4T_1g^{(G)}$	Distorted octahedral
$C_{19}H_{17}ClCoN_2O_5$	299 374 520	1220 220 60	Intra-ligand π → π*, n→π* C.T $^4T_1g^{(F)} \rightarrow {}^4T_1g^{(P)}$	Distorted octahedral
$C_{19}H_{17}ClNiN_2O_5$	241 317 498	2006 230 29	Intra-ligand π → π*, n→π* C.T $^3A_2g^{(F)} \rightarrow 3T_1g^{(F)}$	Distorted octahedral
$C_{19}H_{17}ClCuN_2O_5$	255 386 564	1550 260 90	Intra-ligand π → π*, n→π* C.T $^2B_1g \rightarrow {}^2A_2g$	Distorted octahedral

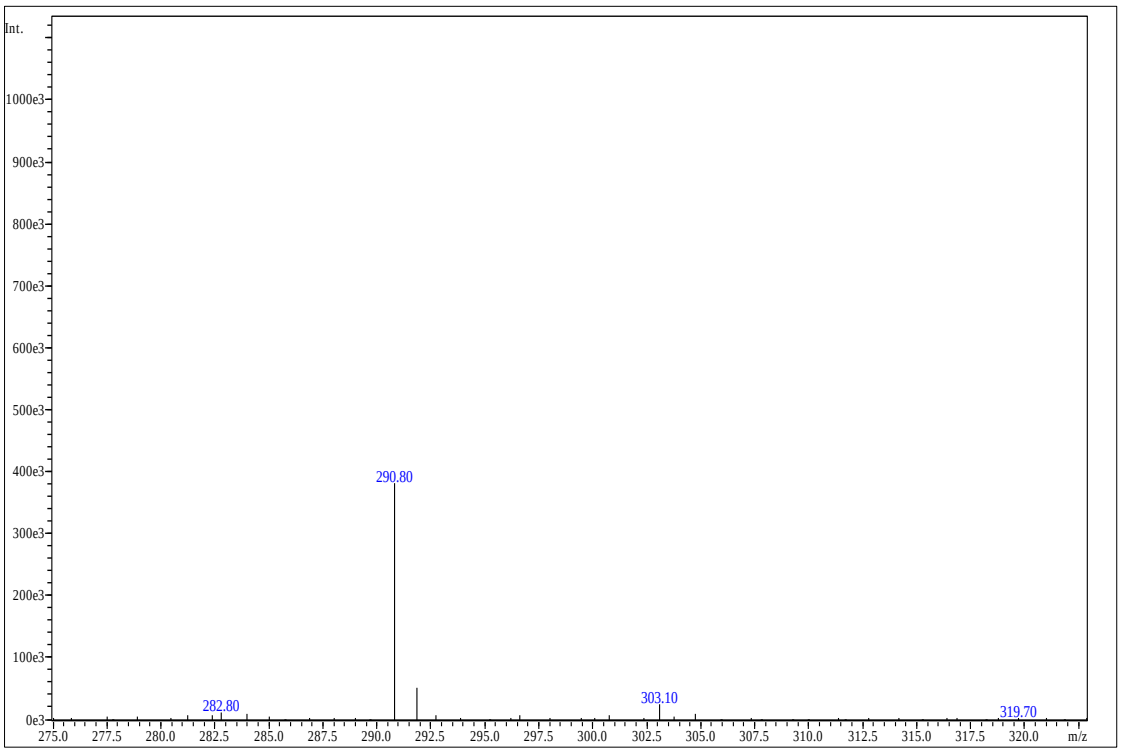

Figure 5: The ESI (+) mass spectrum of azo ligand.

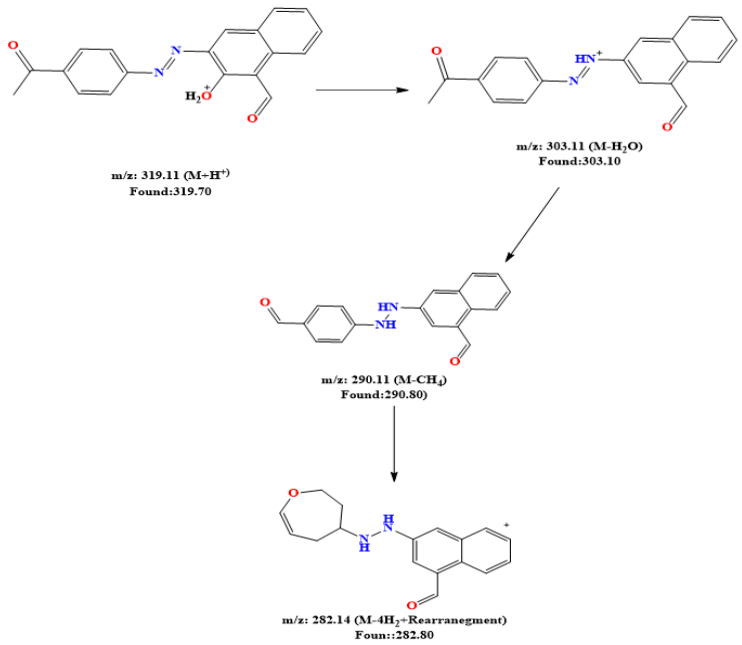

Figure 6: The fragmentation pattern of azo ligand.

Table 5: It shows the areas of antibacterial activity (mm) for HL and compounds.

Compounds	Bacillus cereus (G+)	Staphylococcus aureus (G+)	Proteus mirabilis (G−)	Escherichia coli (G−)
DMSO	-	-	-	-
Tetracycline	30	27	14	1
HL	14	9	10	9
$C_{19}H_{15}Cl_2CrN_2O_4$	14	17	18	22
$C_{19}H_{17}ClMnN_2O_5$	10	9	11	9
$C_{19}H_{17}ClCoN_2O_5$	17	18	18	20
$C_{19}H_{17}ClNi\ N_2O_5$	14	9	11	9
$C_{19}H_{17}ClCuN_2O_5$	16	17	18	17

5.2 Mass Spectrum

Mass spectrum HL was obtained by electron scattering positive mass spectroscopy, spectrum in Figure 5 showed the presence of a parent ion molecule $(M+H)^+$ at m/z = 319amu (2%), measured for $C_{19}H_{14}N_2O_3$, which requires 318.33 amu. Figure 6 showed the fragmentation pattern of azo ligand.

5.3 Electronic Spectra and Magnetic Moment

Magnetic moment and UV-visible is summarised in Table 4. Electron spectrum of the complexes displayed characteristic peaks in the range 241-301 nm, indicating transitions π→π* and n→π*. Further, Charge transfer phenomena are allow for the observed peaks in an array between 316-436 nm. [30,31]. The electron spectra of the Cr(III) complex exhibit a special band at 512 nm, indicative of the transition $^4A_2g \rightarrow {}^2T_1g$, indicating that a distorted octahedral structure around the Cr(III) centre. This explanation agrees to the value of magnetic moment: (3.81) BM for the Cr(III) complex. The Mn(II) complex exhibits a band at 488 nm in the region of d-d, ascribed to the transition $^6A_1g \rightarrow {}^4T_1g(G)$, indicating the geometry around the Mn ion was distorted octahedral. This result corresponds to the magnetic moment measurement for the Mn(II) complex: (5.90) BM. For the Co(II) complex, the spectrum exhibits bands at 520 nm of the d-d region

that correspond with the transition $^4T_1g^{(F)} \rightarrow {}^4T_1g^{(P)}$. A six-coordinate complex suggested by these bands indicates a distorted geometry around the ion of Co(II). The value of magnetic moment: (4.62) BM, agree an octahedral arrangement around the Co ion [30], [32]. Ni(II) complex shows a peak at 498 nm, assigned to $^3A_2g^{(F)} \rightarrow {}^3T_1g^{(P)}$, indicating octahedral geometry around the Ni atom. The value of the magnetic moment: (3.29) BM confirms the octahedral geometry around the Ni ion. Finally, The Cu(II) complex has a peak at 564 nm, ascribed to the $^2B_1g \rightarrow {}^2A_2g$ transition, which suggests a distorted octahedral structure surrounding the ion Cu. The magnetic moment value for ion Cu(II): (1.93) BM is consistent with this structural interpretation [30], [32].

5.4 Biological Activity

By using *Tetracycline* as a reference medication. were utilised four bacterial strains to evaluate the antibacterial activity of the synthesised ligand along with their metal complexes: *(Escherichia coli and Proteus mirabilis (G−))* and also (*Staphylococcus aureus and Bacillus cereus (G+))*. Control experiments separately using dimethyl sulfoxide showed the absence of any intrinsic antibacterial effects [33]-[35]. Table 5 shows the inhibiting area's diameters have been in comparison with those of the antibiotic Syntriaxone. The main results were:

1) HL shows antibacterial activity against (Escherichia coli and Proteus mirabilis (G−)), (Staphylococcus aureus and Bacillus cereus (G+)).
2) The (C19H17ClCoN2O5), (C19H17ClCuN2O5) and (C19H15Cl2CrN2O4) showed stronger effectiveness against selected strains.
3) The metal complexes of HL exhibited significant antibacterial activity comparable to Tetracycline. This might result in potential biological uses of the synthesised compounds.

Antifungal testing has been performed on the yeast (*Candida albicans*), utilising *fluconazole* as the reference medication. DMSO controls did not exhibit antifungal activity [36]-[39]. The observed antifungal activity. The values for the tested substances have been shown in Table 6. The subsequent findings have been discerned;

1) against Candida albicans. All substances exhibited antifungal activity.
2) Complexity substantially enhanced antifungal activity of the free ligand, possibly as a result of the chelate process.
3) Fluconazole has shown greater effectiveness than complexes against Candida albicans.

Table 6: The demonstrates of antifungal inhibition (mm) zones of azo ligand and the compounds.

Compounds	*Candida albicans*
DMSO	-
Fluconazole	9
HL	14
$C_{19}H_{15}Cl_2CrN_2O_4$	17
$C_{19}H_{17}ClMnN_2O_5$	15
$C_{19}H_{17}ClCoN_2O_5$	12
$C_{19}H_{17}ClNi\ N_2O_5$	14
$C_{19}H_{17}ClCuN_2O_5$	16

6 CONCLUSIONS

The azo ligand (HL) and its paramagnetic complexes involving the metals Cr(III), Mn(II), Co(II), Ni(II) and Cu(II) have been reported. The synthesised ligand HL from reaction of the 4-aminoacetophenone with 2-hydroxynaphthalene-1-carbaldehyde in mole ratio one-to-one. The interaction of ligand with metal ions at a (one-to-one) L-to-M ratio generated isolated compounds. They have been structurally characterised via several Physical and chemical techniques. The six-coordinate geometries for the metal complexes' coordination environments given by analytical techniques involve elemental microanalysis,1H and 13C-nuclear magnetic resonance, Fourier transform infrared spectroscopy, electronic and mass spectroscopy, as well as magnetic susceptibility, Conductivity measurements and Biological Evaluation. The ligand Prepared had yield: (72.10%), having a melting point among 136-138□C, As for the complexes resulting from the reaction of the ligand with metal chlorides, the melting point was higher than 300□C. The FTIR of HL displayed characteristic peaks for phenolic, carbonyl, and azo groups. Complexation resulted in carbonyl peak shifts, indicating back-bonding, with additional bands related to the ν(M-N), ν(M-O), ν(M-Cl) and ν(M-OH2) observed in the complex spectra. Mass spectrum of ligand showed the presence of a parent ion molecule (M+H)+ at m/z = 319amu, measured for C19H14N2O3, which requires 318.33 amu. The UV/Vis of complexes supported a distorted octahedral structure. The value of magnetic moment is 3.81, 5.90, 4.62, 3.29 and 1.93BM for Cr, Mn, Co, Ni and Cu, respectively, this explanation agrees to the electron spectra of the complexes. At last, anti-bacterial and anti-fungal

assays demonstrated enhanced bioactivity for the resulting complexes comparing to free ligand, emphasising the plus-side outcomes of complex formation.

REFERENCES

[1] V. M. Dembitsky, T. A. Gloriozova, and V. V. Poroikov, "Pharmacological and predicted activities of natural azo compounds," Nat. Prod. Bioprospect., vol. 7, pp. 151–169, 2017.

[2] A. Z. El-Sonbati, G. G. Mohamed, A. A. El-Bindary, W. M. I. Hassan, and A. K. Elkholy, "Geometrical structure, molecular docking, potentiometric and thermodynamic studies of 3-aminophenol azodye and its metal complexes," J. Mol. Liq., vol. 209, pp. 625–634, 2015.

[3] A. A. El-Bindary, M. A. Hussein, and R. A. El-Boz, "Molecular docking, theoretical calculations and potentiometric studies of some azo phenols," J. Mol. Liq., vol. 211, pp. 256–267, 2015.

[4] E. M. Zayed, A. M. Hindy, and G. G. Mohamed, "Molecular structure, molecular docking, thermal, spectroscopic and biological activity studies of bis Schiff base ligand and its metal complexes," Appl. Organomet. Chem., vol. 32, no. 1, p. e3952, 2018.

[5] V. Beral, K. Gaitskell, W. Zheng, C. Hermon, K. Moser, G. Reeves, R. Peto, and F. Sitas, "Ovarian cancer and smoking: Individual participant meta-analysis including 28,114 women with ovarian cancer from 51 epidemiological studies," Lancet Oncol., vol. 13, pp. 946–956, 2012, doi: 10.1016/S1470-2045(12)70322-4.

[6] T. R. Arun and N. Raman, "Antimicrobial efficacy of phenanthrenequinone based Schiff base complexes incorporating methionine amino acid: Structural elucidation and in vitro bio assay," Spectrochim. Acta A Mol. Biomol. Spectrosc., vol. 127, pp. 292–302, 2014.

[7] J. Bell, J. J. Plumb, C. A. Buckley, and D. C. Stuckey, "Treatment and decolorization of dyes in an anaerobic baffled reactor," J. Environ. Eng., vol. 126, no. 11, pp. 1026–1032, 2000.

[8] K. T. Chung, "Azo dyes and human health: A review," J. Environ. Sci. Health C, vol. 34, no. 4, pp. 233–261, 2016.

[9] S. Benkhaya, S. M'rabet, and A. El Harfi, "Classifications, properties, recent synthesis and applications of azo dyes," Heliyon, vol. 6, no. 1, 2020.

[10] A. Tupys, J. Kalembkiewicz, Y. Ostapiuk, V. Matiichuk, O. Tymoshuk, E. Woźnicka, and Ł. Byczyński, "Synthesis, structural characterization and thermal studies of a novel reagent 1-[(5-benzyl-1,3-thiazol-2-yl) diazenyl] naphthalene-2-ol," J. Therm. Anal. Calorim., vol. 127, pp. 2233–2242, 2017.

[11] A. Penchev, D. Simov, and N. Gadjev, "Diazotization of 2-amino-6-methoxybenzothiazole at elevated temperature," Dyes Pigm., vol. 16, no. 1, pp. 77–81, 1991.

[12] G. B. Bagihalli, P. G. Avaji, S. A. Patil, and P. S. Badami, "Synthesis, spectral characterization, in vitro antibacterial, antifungal and cytotoxic activities of Co(II), Ni(II) and Cu(II) complexes with 1,2,4-triazole Schiff bases," Eur. J. Med. Chem., vol. 43, no. 12, pp. 2639–2649, 2008.

[13] N. Aggarwal, R. Kumar, P. Dureja, and D. S. Rawat, "Schiff bases as potential fungicides and nitrification inhibitors," J. Agric. Food Chem., vol. 57, no. 18, pp. 8520–8525, 2009.

[14] C. Liu, W. Zhang, and G. Cai, "Synthesis, crystal structures and catalytic activities of two copper coordination compounds bearing an N,N'-dibenzylethylenediamine ligand," Crystals, vol. 10, no. 6, p. 528, 2020.

[15] B. K. Al-Rubaye, M. J. Al-Jeboori, and H. Potgieter, "Metal Complexes of Multidentate N2S2 Heterocyclic Schiff-base Ligands; Formation, Structural Characterisation and Biological Activity," J. Phys. Conf. Ser., vol. 1879, no. 2, p. 022074, 2021.

[16] H. J. Abaas and M. J. Al-Jeboori, "New dimeric complexes with semicarbazone Mannich-based ligand; formation, structural investigation and biological activity," Rev. Bionatura, vol. 8, no. 2, p. 15, 2023.

[17] J. Conradie, M. M. Conradie, Z. Mtshali, D. van der Westhuizen, K. M. Tawfiq, M. J. Al-Jeboori, S. J. Coles, C. Wilson, and J. H. Potgieter, "Synthesis, characterisation and electrochemistry of eight Fe coordination compounds containing substituted 2-(1-(4-R-phenyl-1H-1,2,3-triazol-4-yl)pyridine ligands, R = CH3, OCH3, COOH, F, Cl, CN, H and CF3," Inorg. Chim. Acta, vol. 484, pp. 375–385, 2019.

[18] H. Kocaokutgen and E. Erdem, "Synthesis and spectral characterization of metal complexes of 1-(2-Hydroxy-4-methylphenylazo)-2-naphthol," Synth. React. Inorg. Met.-Org. Chem., vol. 34, no. 10, pp. 1843–1853, 2004.

[19] K. Y. Law, I. W. Tarnawskyj, and P. T. Lubberts, "Azo pigments and their intermediates: Effect of substitution on the diazotization and coupling reactions of o-hydroxyanilines," Dyes Pigm., vol. 23, no. 4, pp. 243–254, 1993.

[20] A. J. Jarad, M. A. Dahi, T. H. Al-Noor, M. M. El Ajaily, S. R. Al-Ayash, and A. Abdou, "Synthesis, spectral studies, DFT, biological evaluation, molecular docking and dyeing performance of 1-(4-((2-amino-5-methoxy) diazenyl) phenyl) ethanone complexes with some metallic ions," J. Mol. Struct., vol. 1287, p. 135703, 2023.

[21] E. J. Baron and S. M. Finegold, Diagnostic Microbiology, 8th ed. London, U.K.: Mosby Company, 1990, pp. 53–62.

[22] S. A. Hussein and E. I. Yousif, "New mannich base (2R)-4-methyl-2-((S)(phenylamino)(p-tolyl) methyl) cyclohexan-1-one; synthesis and spectral characterisation," J. Phys. Conf. Ser., vol. 1, p. 012019, 1999.

[23] H. A. Hasan, W. M. Alwan, R. M. Ahmed, and E. I. Yousif, "Synthesis and characterization of some mixed-ligand complexes containing azo dye and 1,10-phenanthroline with (CoII, ZnII, CdII and HgII ions)," Ibn Al-Haitham J. Pure Appl. Sci., vol. 28, no. 3, pp. 187–203, 2015.

[24] A. A. Ismail and S. M. Lateef, "Synthesis of novel complexes of VO(II), Mn(II), Fe(II), Co(II), Ni(II), Cu(II) and Pt(IV) derived from Schiff's base of pyridoxal and 2-amino-4-nitrophenol and study of their biological activities," Ibn Al-Haitham J. Pure Appl. Sci., vol. 36, no. 2, pp. 259–275, 2023.

[25] B. K. Mohammed and E. I. Yousif, "Synthesis, structural characterisation and biological activity of new metal complexes derived from semicarbazone ligand," Rev. Bionatura, vol. 8, no. 2, p. 14, 2023.

[26] A. C. Olivieri, R. B. Wilson, I. C. Paul, and D. Y. Curtin, "Carbon-13 NMR and x-ray structure determination of 1-(arylazo)-2-naphthols. Intramolecular proton transfer between nitrogen and oxygen atoms in the solid state," J. Am. Chem. Soc., vol. 111, no. 15, pp. 5525–5532, 1989.

[27] L. Guasch, W. Yapamudiyansel, M. L. Peach, J. A. Kelley, J. J. Barchi Jr., and M. C. Nicklaus, "Experimental and chemoinformatics study of tautomerism in a database of commercially available screening samples," J. Chem. Inf. Model., vol. 56, no. 11, pp. 2149–2161, 2016.

[28] L. Racane, Z. Mihalić, H. Cerić, J. Popović, and V. Tralić-Kulenović, "Synthesis, structure and tautomerism of two benzothiazolyl azo derivatives of 2-naphthol: A crystallographic, NMR and computational study," Dyes Pigm., vol. 96, no. 3, pp. 672–678, 2013.

[29] P. M. Tolstoy, J. Guo, B. Koeppe, N. S. Golubev, G. S. Denisov, S. N. Smirnov, and H. H. Limbach, "Geometries and tautomerism of OHN hydrogen bonds in aprotic solution probed by H/D isotope effects on 13C NMR chemical shifts," J. Phys. Chem. A, vol. 114, no. 40, pp. 10775–10782, 2010.

[30] E. Ramachandran, V. Gandin, R. Bertani, P. Sgarbossa, K. Natarajan, N. S. Bhuvanesh, A. Venzo, A. Zoleo, A. Glisenti, A. Dolmella, and A. Albinati, "Synthesis, characterization and cytotoxic activity of novel copper(II) complexes with aroylhydrazone derivatives of 2-oxo-1,2-dihydrobenzo[h]quinoline-3-carbaldehyde," J. Inorg. Biochem., vol. 182, pp. 18–28, 2018.

[31] A. B. P. Lever, Inorganic Electronic Spectroscopy, 2nd ed., 1984.

[32] R. V. Singh, R. Dwivedi, and S. C. Joshi, "Synthetic, magnetic, spectral, antimicrobial and antifertility studies of dioxomolybdenum(VI) unsymmetrical imine complexes having a N∩N donor system," Transit. Met. Chem., vol. 29, no. 1, pp. 70–74, 2004.

[33] R. Ramesh and S. Maheswaran, "Synthesis, spectra, dioxygen affinity and antifungal activity of Ru(III) Schiff base complexes," J. Inorg. Biochem., vol. 96, pp. 457–462, 2003.

[34] A. Rahman, M. Choudhary, and W. Thomsen, Bioassay Techniques for Drug Development. Amsterdam, The Netherlands: Harwood Academic, 2001.

[35] M. J. Al-Jeboori, E. I. Abdulkarim, and S. Attia, "Synthesis and Characterization of Novel Ligand Type N2O2 and its Complexes with Cu(II), Co(II), Ni(II), Zn(II), and Cd(II) ions," Ibn Al-Haitham J. Pure Appl. Sci., vol. 18, no. 2, pp. 51–67, 2015.

[36] M. J. Al-Jeboori, A. T. Numan, and D. J. Ahmed, "Synthesis and Characterisation of Novel Cobalt(II), Copper(II) and Mercury(II) Complexes of Poly Vinyl Urethanised Oxime," Ibn Al-Haitham J. Pure Appl. Sci., vol. 21, no. 2, pp. 89–101, 2017.

[37] H. M. Salh and T. H. Al-Noor, "Preparation, structural characterization and biological activities of curcumin-metal(II)-L-3,4-dihydroxyphenylalanin(L-dopa) complexes," Ibn Al-Haitham J. Pure Appl. Sci., vol. 36, no. 1, 2023.

[38] A. S. A. K. A. Rahman, N. J. Hussien, K. T. Abdullah, S. F. M. Yusof, and E. I. Yousif, "Synthesis, characterization and antibacterial activity of some transition metal complexes of a new dioxime ligand," AIP Conf. Proc., vol. 2593, p. 060001, 2023.

[39] S. A. Hussain and M. J. Al-Jeboori, "New metal complexes derived from Mannich-base ligand; Synthesis, spectral characterisation and biological activity," J. Global Pharma Tech, vol. 11, no. 2, pp. 548–560, 2019.